# ON THE PRECIPITATION HARDENING OF SELECTIVE LASER MELTED AlSi10Mg

Nesma T. Aboulkhair[a*], Chris Tuck[b], Ian Ashcroft[b], Ian Maskery[b], Nicola M. Everitt[a]

[a] Materials, Mechanics and Structures Research Division, Faculty of Engineering, University of Nottingham, Nottingham NG7 2RD, United Kingdom

[b] Manufacturing and Process Technologies Research Division, Faculty of Engineering, University of Nottingham, Nottingham NG7 2RD, United Kingdom

Precipitation hardening of selective laser melted AlSi10Mg was investigated in terms of solution heat treatment and aging duration. The influence on the microstructure and hardness was established, as was the effect on the size and density of Si particles. Although the hardness changes according to the treatment duration, the maximum hardening effect falls short of the hardness of the as-built parts with their characteristic fine microstructure. This is due to the difference in strengthening mechanisms.

**Keywords:** Selective laser melting, aluminum alloys, heat treatment, microstructure, hardness

Additive manufacturing (AM) techniques are under extensive investigation for their potential to replace conventional manufacturing methods in the production of complex structures. Selective laser melting (SLM) is an AM technology for the production of metal parts from powders using a high intensity infra-red laser [1, 2]. Several researchers are interested in material qualification studies for Al alloys in this field [3, 4], and there are numerous studies paying special attention to the mechanical properties of parts manufactured from Al alloys by SLM such as hardness [5, 6], tensile behavior [4, 6-9], creep resistance [4], impact energy [6], and fatigue [10]. In most of these studies a heat treatment has been employed with the aim of enhancing the mechanical behavior of the parts. For the AlSi10Mg alloy, the alloy of interest in this study, annealing is usually used to promote ductility whereas it is conventionally strengthened through precipitation hardening. Precipitation hardening for AlSi10Mg is divided into two steps; (1) solution heat treatment (SHT) followed by quenching and (2) artificial aging (AA) at 423-453 K (150-180 °C) [11]. Each step is conducted over duration of time, which is generally provided as a range. The durations are based on studies conducted on conventionally manufactured components from AlSi10Mg that have microstructures that are entirely different from that developed during the SLM process [3]. The duration for each step is of crucial importance to avoid underaging or overaging, which has consequent results in reducing hardness. An example of the importance of the aging process has been shown by Brandl *et al*. [10] where the fatigue resistance of AlSi10Mg SLM parts was enhanced following a hardening regime. However, whether Brandl *et al*. [10] selected the most appropriate SHT and AA durations for optimal fatigue resistance requires further investigation. Prashanth *et al*. [9] reported a mechanical properties dependence on the microstructure evolution of selective laser melted Al-12Si during annealing at different temperatures. Understanding the unique microstructure produced by SLM and its response to precipitation hardening (in hardenable alloys) is essential at this point. This paper shows a method of identifying the optimal heat treatment conditions; SHT and AA for AlSi10Mg for the purposes of optimizing the hardness of components manufactured using SLM. To the authors' knowledge, there is no study so far in the literature that has explored this issue thoroughly.

In this study, SLM samples were manufactured from AlSi10Mg powder supplied by LPW Technology (UK) using a Renishaw AM250 SLM machine (UK) equipped with a 200 W Yb-Fibre laser ($\lambda$=1064 nm). Samples were processed using a hatch spacing of 0.08 mm and a scan speed of 318 mm/s. The samples were heat treated by precipitation hardening (T6) in the following sequence: (1) SHT at 793 K (520 °C) for 1, 2, 3, and 4 hrs; (2) water quenching; and (3) AA at 433 K (160 °C) for 6, 8, 10, and 12 hrs followed by air cooling.

* Corresponding author: emxntab@nottingham.ac.uk

The samples were polished and immersed in Keller's etchant for 20-25 seconds to reveal their microstructures. Using a Nikon Eclipse LV100ND microscope, the microstructure of the as-built sample (see the isometric view in Figure 1(a)) was observed in the planes perpendicular and parallel to the build direction (referred to hereafter as XY and XZ planes, respectively) as shown in Figures 1(b) and (c). The grains in the XY plane are equiaxed (cellular grains) whereas in the XZ plane they are elongated (columnar) in the direction of thermal gradient. This is the characteristic microstructure for SLM parts as has been previously reported [3, 5]. A Phillips XL30 scanning electron microscope (SEM) with a 20 kV accelerating voltage equipped with an energy dispersive x-ray (EDX) detector was used for additional imaging and chemical composition analysis. EDS confirmed that during solidification Si particles segregate at the Al grain boundaries (see Figure 2). Fast cooling reduces the amount of Si rejected into the liquid by extending the solubility of Si in Al [12], so α-Al solidifies first in the preferential cellular structure leaving the residual Si at the grain boundaries [9]. When the material was solution heat treated for 1 hr (Figure 1(d)) the microstructure coarsened and Si started diffusing to form particles instead of being segregated around the grain boundaries of the α-Al. Further increases in the SHT duration promoted diffusion, leading to larger particles (see Figure 1(e)). Agglomerates of Si particles were observed at the melt pool boundaries. The preferential growth of Si particles at the melt pool boundaries could be seen because these regions were remelted more than once during processing since they lie at the overlap of two hatches. SHT for more than two hours significantly dissolved the scan tracks even before aging, as shown in Figure 1(e) for the sample that underwent SHT for 4 hrs. The scan tracks that were not dissolved during SHT diminished upon aging, yielding a more homogenous microstructure (Figures 1(f) and (g)).

The observations made from the micrographs of the samples treated for different durations (Figure 1) were further supported by analyzing the size of the Si particles and their spatial density (using the open source software ImageJ 1.46r [13]), as demonstrated in Figure 3. The particles' size and density for the as-built samples could not be quantified since the alloying elements were found as continuous segregations at the grain boundaries without a definite shape. However, at the early stages of SHT (1 hr), particles started to form with a specific size and density. As the SHT progressed, the average particle size increased until it reaches a plateau in the range of 3-4 hrs, with average Si particle sizes of 1.40 and 1.42 μm, respectively. The spatial density of the particles decreased with increasing SHT duration since the particles diffuse to form larger particles, but the quantity of Si remains constant. When all samples subjected to different SHT durations were aged for 6 hrs, it was observed that the Si particle size and density were not significantly altered. The particles' size and density started to change with further aging. It is important to note that during heat treatment, not only particle diffusion or dissolution occurred but also nucleation sites for the formation of needle-like $Mg_2Si$ precipitates were observed (see Figures 1(f) and (g)) that are expected to influence the particulate measurements. In addition, a fraction of these precipitates might not be adequately represented because their size is below the threshold of the image's resolution. Nevertheless they will be contributing to the overall hardness.

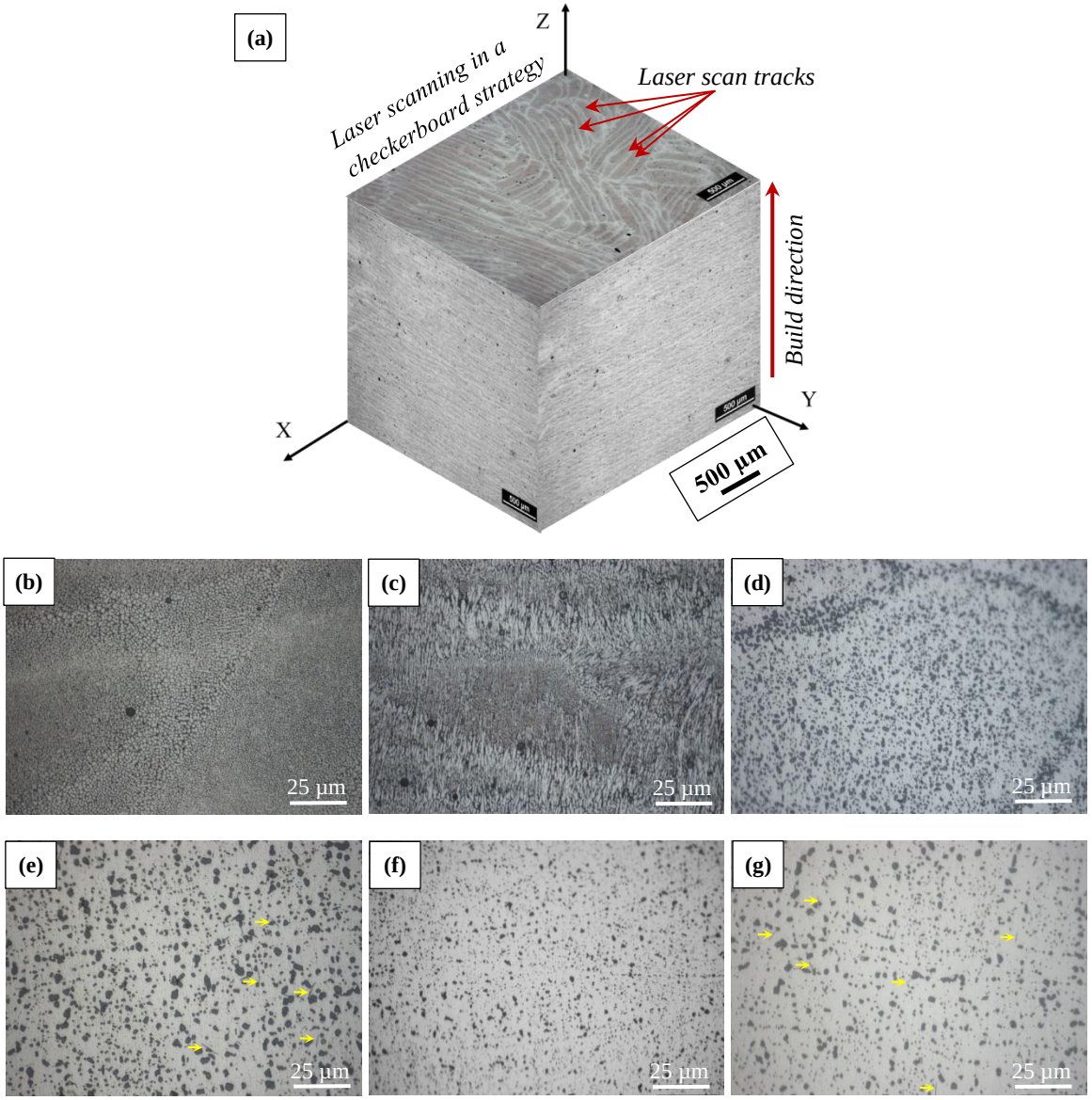


Figure 1: (a) An isometric view showing the 3 views of an SLM cube in addition to high magnification micrographs for the microstructure of (b) as-built XY plane, (c) as-built XZ plane, (d) XY plane after 1 hr SHT, (e) XZ plane after 4 hrs SHT, (f) XZ plane after 1 hr SHT and 12 hrs AA, and (g) XZ plane after 4 hrs SHT and 6 hrs AA with arrows pointing toward nucleation sites for needle-like $Mg_2Si$ precipitates.

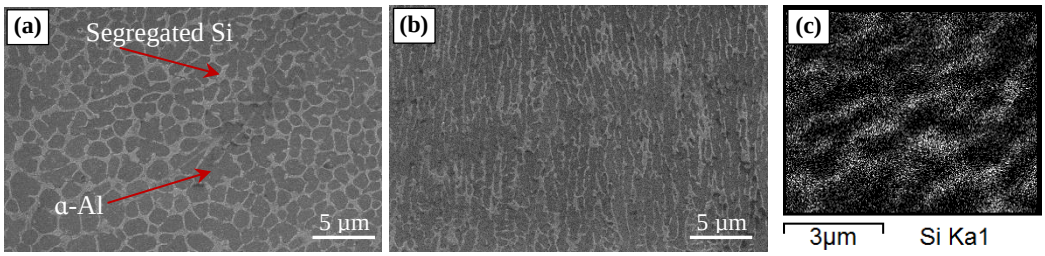


Figure 2: Microstructure of (a) as-built sample XY plane, (b) as-built sample XZ plane, and (c) EDS composition map for Si (white pixels) in the as built sample XY plane.

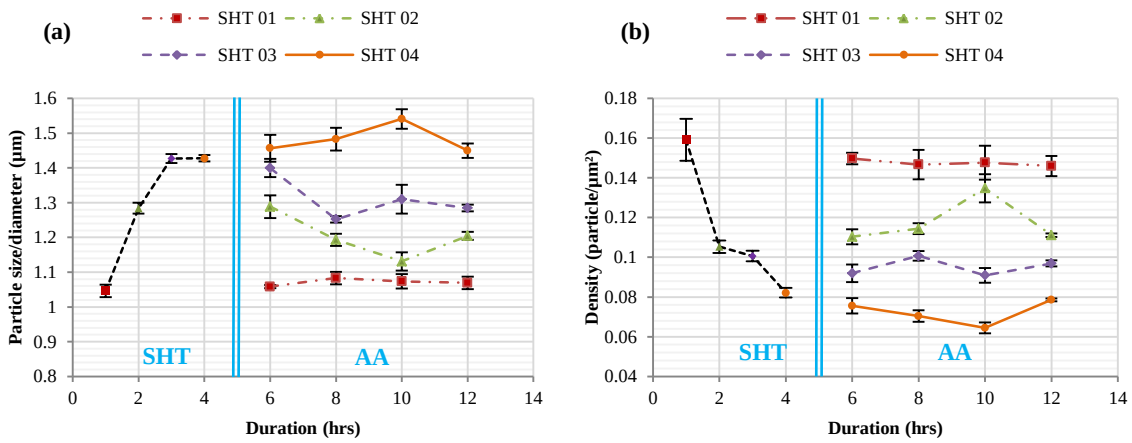


Figure 3: Particles analysis showing change in (a) average particle size and (b) particle density with heat treatment duration with error bars representing the standard error.

Hardness tests were conducted using a Vickers hardness tester with a load of 300 gf. The hardness of the prepared samples was expected to be influenced by the microstructure developed at different heat treatment durations. The evolution of hardness with changing the heat treatment procedure can be found in Figure 4. The highest hardness was achieved with the as-built selective laser melted material. The material was significantly softened by SHT for one hour due to microstructure coarsening. Hardness started to increase with further increase in SHT duration. This could be attributed to the increase in the size of the Si particles as described above. Hardness then increased when the material was artificially aged due to the formation of $Mg_2Si$ precipitates. However, it is quite noticeable that the maximum enhancement in hardness falls short compared to the as-built material; losing 12.3% of the original hardness. This is better understood by considering the various strengthening mechanisms in both the as-built and heat treated material. In the as-built material, hardness or strength is mainly attributed to: (1) grain size reduction governed by the Hall-Petch equation $\sigma_y = \sigma_0 + k\,(d)^{-1/2}$, where $\sigma_y$ is the yield strength, $\sigma_0$ is a material constant denoting the stress required to start dislocation motion, K is the strengthening coefficient, and d is the grain size, (2) solid solution strengthening due to the presence of alloying elements, and (3) dislocation strengthening through the interaction of dislocations impeding each other's motion. On the other hand, strengthening in the case of precipitation hardening is dominated by the presence of precipitates or dispersoids, referred to as Orowan strengthening, in addition to the solid solution strengthening and dislocation strengthening [14]. In as-built samples the dislocation motion is mainly hindered by the increased volume of grain boundaries whereas in the hardened material the dislocation motion is obstructed by the dispersoids acting as obstacles. For overaged materials, the strength decreases because the precipitates are bypassed by the dislocation, depressing the effect of Orowan strengthening [15]. This is because the increase in precipitate size would require more energy from the dislocation to shear through so bypass is promoted [16]. The presence of precipitates in aged alloys is known to boost the material's hardness. This was evident in this study when comparing the samples subjected to SHT to those aged. However, this was not the case when comparing aged samples to as-built. This indicates that the effect of grain boundary strengthening (through grain size reduction) in the as-built samples outweighed the contribution of Orowan strengthening by the presence of dispersoids in the aged samples.

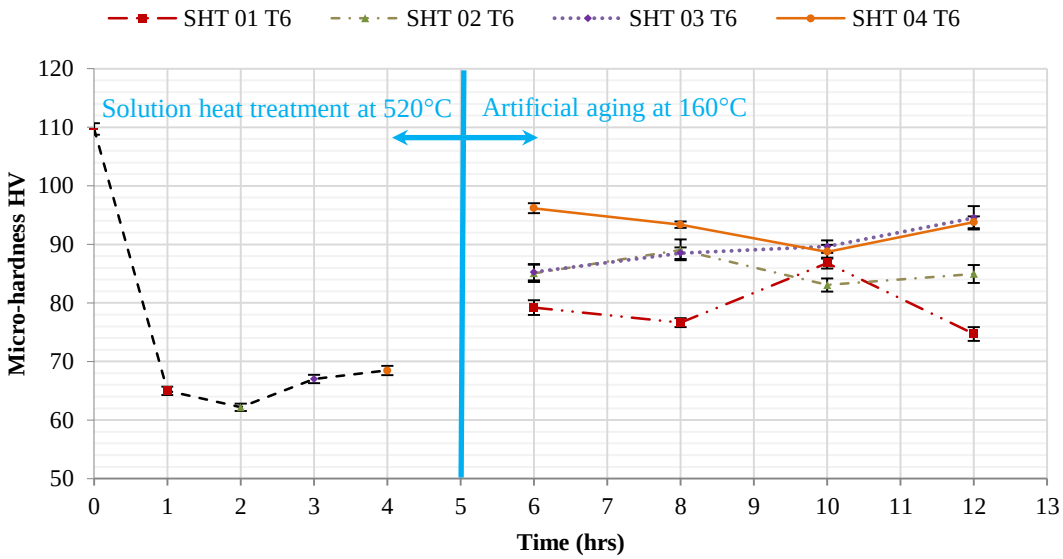


Figure 4: Evolution of micro-hardness with heat treatment procedure with error bars representing the standard error.

The importance of this study lies within the difference between the response of conventionally manufactured (e.g. casting) Al alloys and those fabricated by SLM. The response is typically a function of the microstructure. A comparison between both materials' microstructures and responses is presented in Table 1. It has been previously reported that the aging response of Al-Si-Mg alloys is independent of the SHT time in the case of casting [17]. However, the results discussed here showed that this is not the case for SLM materials, since the SHT duration was found to significantly influence the aging response as represented by the material's hardness. Moreover, the fineness of the microstructure dominates the selection of SHT times. For cast alloys, shorter times of SHT are needed to completely homogenize finer microstructures [18], but the characteristically fine microstructure of SLM parts required longer SHT durations to stabilize the microstructure and enhance the mechanical response with and without aging. Precipitation behavior in coarse-grained Al alloys differs from that in ultrafine-grained Al alloys [19]. Consequently, when dealing with Al alloys processed by SLM, it is crucial to bear in mind that it is an ultrafine-grained material rather than a conventional coarse-grained.

Table 1: Comparing the microstructure of SLM AlSi10Mg and its conventionally cast counterpart with and without precipitation hardening.

| **Point of comparison** | **SLM material** | **Conventional cast material** |
|---|---|---|
| As-fabricated | Fine microstructure with continuous Si segregations on the grain boundaries of α-Al | Coarse dendritic microstructure [18] with Si in the form of flakes [20] |
| Precipitation hardening | Microstructure coarsens to become a solid solution of Si particles in a matrix of α-Al | Fine Si particles form and cluster at the grain boundaries of α-Al [20], generally a globular microstructure. |
| Precipitation hardening effect on hardness | Hardness decreased for the investigated range | Hardness increases until peak hardening (~10 hrs AA) then decreases with over aging [21] |

The current study is a first step in the development of a T6 treatment for SLM Al-Si alloys considering only the response of hardness to the different precipitation hardening procedures. Further investigations on other mechanical properties are underway and will be the subject of future publications. Investigation of a larger range of AA temperatures will also be conducted. Although the focus of this paper was on precipitation hardening, other heat treatment procedures require attention as well given the characteristic microstructure of Al parts processed by SLM. This microstructure might require developing tailored heat treatment procedure to yield the mechanical behavior needed in operation.

## Acknowledgements

Nesma T. Aboulkhair gratefully acknowledges funding provided by the Dean of Engineering Scholarship for International Research Excellence, Faculty of Engineering, University of Nottingham.

## References

[1] B. Ferrar, L. Mullen, E. Jones, R. Stamp, and C. J. Sutcliffe, J. Mater. Process. Technol., 2012, vol. 212, pp. 355-364.

[2] D. Dai and D. Gu, Mater. Des., 2014, vol. 55, pp. 482-491.

[3] N. T. Aboulkhair, N. M. Everitt, I. Ashcroft, and C. Tuck, Addit. Manuf., 2014, vol. 1-4, pp. 77-86.

[4] N. Read, W. Wang, K. Essa, and M. Attallah, Mater. Des., 2015, vol. 65, pp. 417-424.

[5] L. Thijs, K. Kempen, and J-P. Kruth, Acta. Mater., 2013, vol. 61, pp. 1809-1819.

[6] K. Kempen, L. Thijs, J. Humbeeck, and J-P. Kruth, Phys. Procedia, 2012, vol. 39, pp. 439-446.

[7] D. Buchbinder, H. Schleifenbaum, S. Heidrich, W. Meiners, and J. Bültmann, Phys. Procedia, 2011, vol. 12, pp. 271-278.

[8] X. J. Wang, L. C. Zhang, M. H. Fang, and T. B. Sercombe, Mater. Sci. Eng. A, 2013, vol. 597, pp. 370-375.

[9] K. G. Prashanth, S. Scudino, H. J. Klauss, K. B. Surreddi, L. Löber, Z. Wang, A. K. Chaubey, U. Kühn, and J. Eckert, Mater. Sci. Eng. A, 2014, vol. 590, pp. 153-160.

[10] E. Brandl, U. Heckenberger, V. Holzinger, and D. Buchbinder, Mater. Des., 2013, vol. 34, pp. 159-169.

[11] T. V. Rajan, C. P. Sharma, and A. Sharma, Heat Treatment: Principles and Techniques, second ed., PHI Learning Limited, New Delhi, 2011.

[12] S. K. Bose and R. Kumar, J. Mater. Sci., 1973, vol. 8, pp. 1795-1799.

[13] M. D. Abramoff, P. J. Magalhaes, and S. J. Ram, Biophotonics. Int., 2004, vol. 11, pp. 7.

[14] K. Ma, H. Wen, T. Hu, T. D. Topping, D. Isheim, D. N. Seidman, E. J. Lavernia, and J. M. Schoenung, Acta. Mater., 2014, vol. 62, pp. 141-155.

[15] J. F. Nie and B. C. Muddle, Mater. Sci. Eng. A, 2001, vol. 319-321, pp. 448-451.

[16] E. Sjölander and S. Seifeddine, J. Mater. Process. Technol., 2010, vol. 210, pp. 1249-1259.

[17] E. Sjölander and S. Seifeddine, Mater. Sci. Eng. A, 2011, vol. 528, pp. 7402-7409.

[18] E. Sjölander and S. Seifeddine, Mater. Des., 2010, vol. 31, pp. S44-S49.

[19] T. Hu, K. Ma, T. D. Topping, J. M. Schoenung, and E. J. Lavernia, Acta. Mater., 2013, vol. 61, pp. 2163-2178.

[20] S. Wisutmethangoon, S. Thongjan, N. Mahathaninwong, T. Plookphol, and J. Wannasin, Mater. Sci. Eng. A, 2012, vol. 532, pp. 610-615.

[21] H.C. Long, J.H. Chen, C.H. Liu, D.Z. Li, and Y.Y. Li, Mater. Sci. Eng. A, 2013, vol. 556, pp. 112-118.